Journal of the Korean Astronomical Society
53: 117 ∼ 123, 2020 December

https://doi.org/10.5303/JKAS.2020.53.6.117
pISSN: 1225-4614 · eISSN: 2288-890X
http://jkas.kas.org

Mechanism Inducing Gas Supply to the Central 10 Parsec of the Milky Way

Hannah L. Morgan[1], Sungsoo S. Kim[1,2], Jihye Shin[3], Kyungwon Chun[1,3], So-Myoung Park[1,3], Joowon Lee[1], and Young Chol Minh[3]

[1]School of Space Research, Kyung Hee University, Yongin, Gyeonggi 17104, Korea
[2]Department of Astronomy & Space Science, Kyung Hee University, Yongin, Gyeonggi 17104, Korea
[3]Korea Astronomy and Space Science Institute, Daejeon 34055, Korea

Received August 16, 2020; accepted November 3, 2020

Abstract: We investigate the plausibility of mass return, from stellar mass loss processes within the central ∼100 pc region of the Milky Way (the inner nuclear bulge), as a mass supply mechanism for the Circumnuclear Disk (CND). Gas in the Galactic disk migrates inward to the Galactic centre due to the asymmetric potential caused by the Galactic bar. The inward migration of gas stops and accumulates to form the central molecular zone (CMZ), at 100–200 pc from the Galactic center. It is commonly assumed that stars have formed in the CMZ throughout the lifetime of the Galaxy and have diffused inward to form a 'r^{-2} stellar cusp' within the inner nuclear bulge. We propose that the stars migrating inward from the CMZ supply gas to the inner nuclear bulge via stellar mass loss, resulting in the formation of a gas disk along the Galactic plane and subsequent inward migration down to the central 10 pc region (CND). We simulate the evolution of a gas distribution that initially follows the stellar distribution of the aforementioned stellar cusp, and illustrate the potential gas supply toward the CND.

Key words: Galaxy: center — Galaxy: nucleus — Galaxy: local interstellar matter — Galaxy: evolution

1. Introduction

The Central Molecular Zone (CMZ), spanning the central ∼200 pc of the Milky Way, contains the largest concentration of dense molecular gas in the Galaxy. Observations and theoretical analyses of young massive star clusters suggest that mass supply occurred recently (Pfuhl et al. 2011; Lu et al. 2017). The primary mechanism supplying the majority of the gas to the Circumnuclear Disk (CND), which spans the central ∼10 pc region, is currently unknown and debated (Martins et al. 2007).

Double-barred galaxies account for approximately 30 % of all barred galaxies (Laine et al. 2002), implying that these structures are long-lived or recurrent. Copious double-bars are observed in proximity to the Milky Way (see, e.g., Erwin (2004) and references therein); hence, it has been suggested that the Milky Way contains a secondary bar, which would be advantageous as such systems are considered to increase the mass inflow. Specific components of double-barred galaxies, the dynamics of and interactions between the bars, and the overall effects double bars have on galaxies have been analyzed in previous investigations (Maciejewski & Sparke 2000; El-Zant & Shlosman 2003; Debattista & Shen 2007; Namekata et al. 2009; Maciejewski & Small 2010, etc.). Namekata et al. (2009) performed 2-dimensional hydrodynamic simulations of the gas motions in the central region of a double-barred galaxy and showed inward gas movements from the CMZ region to the CND region. However, their 2-dimensional models neglected the physical effects of star formation, gas heating and cooling, and supernova feedback and their result does not appear to be confirmed by more sophisticated 3-dimensional simulations. In our unpublished study, we have performed 3-dimensional hydrodynamic simulations using parallel N-body/SPH code GADGET-3 (Springel 2005) that includes star formation, heating and cooling, and supernova feedback (Shin et al. 2014, 2017), for gas motions in the central few hundred pc region with the incorporation of an elongated nuclear bulge as a secondary (inner) bar. This investigation did not yield a stable substantial mass inflow rate down to the CND region.[1] In order to fully understand the connection between double bars and mass supply, further investigations are necessary; several other physical components may be required.

Other scenarios for the inflow of gas down to the CND include the infall of a satellite galaxy onto the central region of the Galaxy (Lang et al. 2013; Gallege & Cuadra 2017), and a gas cloud plunging from the inner nuclear bulge to the CND (Wardle & Yusef-Zadeh 2008; Mapelli & Trani 2016; Ballone et al. 2019). However, these scenarios are rather more episodic than sustainable.

Here, we propose an alternative mechanism for supplying mass from the CMZ to the CND and suggest that the stars formed in the CMZ can deliver gas to the CND region via their inward diffusive migration and mass loss

Corresponding author: Sungsoo S. Kim

[1]We note that a study by Gerhard & Martinez-Valpuesta (2012) questions the conjecture on the existence of a secondary nuclear bar in the Milky Way.

during the late phases of stellar evolution. Gradual gas replenishment occurs as the stars undergo stellar mass loss phases and processes. Main-sequence stars with masses smaller than $\sim 8.0\,M_{\odot}$ end in the form of planetary nebulae (PNe), and during the asymptotic giant branch (AGB) and PN phases, these stars return a substantial fraction of their initial mass to the surrounding interstellar medium (ISM) in the form of low velocity stellar winds and outer envelope shock fronts. Some of the gas replenished from these stars in the central $\sim$100 pc (the inner nuclear bulge) region will form a planar structure along the Galactic plane due to the orbital angular momentum of the stellar population, which originates from the CMZ. A fraction of the gas in this planar structure may migrate down to the CND region through several orbital energy loss processes discussed in Section 4.

In the present work, we estimate the gas replenishment rate associated with each returned percentage mass. We then present 3-dimensional hydrodynamic simulations for the evolution of an initially cylindrical distribution of gas in the inner nuclear bulge, using mass loss rates associated with specific PN evolutionary phases.

2. GAS REPLENISHMENT IN THE INNER NUCLEAR BULGE

A fraction of the gas from the Galactic disk falls to the central region of the Galaxy due to the asymmetric gravitational potential of the Galactic bar. Inwardly moving gas particles stop and accumulate to form the CMZ at 100–200 pc from the Galactic center. Morris & Serabyn (1996) assert that star formation has sustained in the CMZ throughout the lifetime of the Galaxy and stars formed there have diffused further inward to form a 'r^{-2} stellar cusp',[2] or a nuclear stellar disk (Launhardt et al. 2002).

Stars that migrate to the inner nuclear bulge replenish most of their gas back to the interstellar space in the form of winds, thermal pulsations, or PNe. However, terminal wind velocities of massive stars may exceed 1,000 km/s, and winds with such high velocities can escape from the inner nuclear bulge (the velocity required for a point mass to reach $r_g = 200$ pc from $r_g = 50$ pc is 230 km/s, where r_g is the 3-dimensional Galactocentric radius). On the other hand, when considering the whole stellar mass spectrum, a considerable amount of the total initial stellar mass is lost during and before the PN phase and the typical expansion velocity of AGB stars that evolve into PNe is only $\sim$40 km/s (Jacob et al. 2013). For these reasons, we will calculate the stellar mass loss rate throughout the AGB/PN phase[3] and use it as the lower limit of the gas replenishment rate in the inner nuclear bulge.

[2] Launhardt et al. (2002) find that the density slope of this cusp is about -2 only for the central $\sim$30 pc and is shallower at larger radii.

[3] The AGB and PN phases of stars that eventually evolve into PNe and white dwarfs.

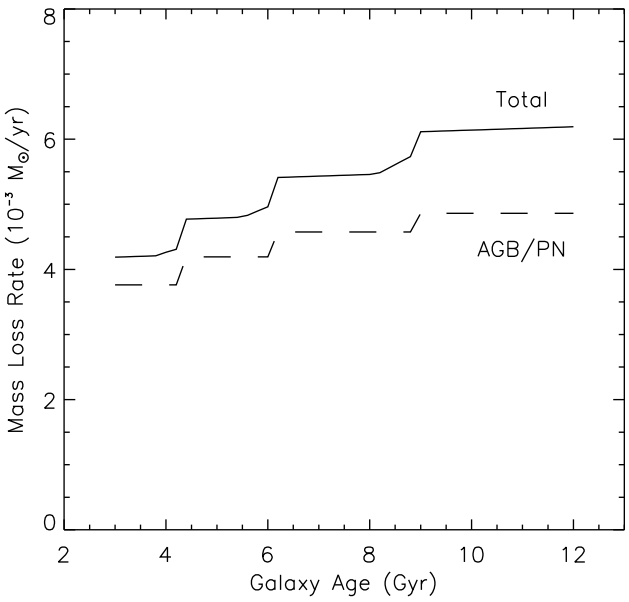

Figure 1. Stellar mass loss rates for a constant SFR of $0.1\,M_{\odot}$/yr for the whole lifetime of the Milky Way as a function of the Galaxy's age. The solid line indicates the total stellar mass loss rate from all stars, the dashed line marks the mass loss rate during the AGB/PN phase from the stars that eventually evolve into PNe and white dwarfs.

To estimate the current stellar mass loss rate, one needs information on the star formation history (SFR), initial mass function (IMF), and stellar evolution model. For the SFR, we assume continuous star formation in the CMZ at a constant rate and adopt $0.1\,M_{\odot}$/yr (Kruijssen et al. 2014). We implement the Kroupa (2002) multipart power-law model for the IMF, and the Hurley et al. (2000) model for stellar evolution. When considering a constant SFR of $0.1\,M_{\odot}$/yr over 12 Gyrs, we obtain $1.1 \times 10^9\,M_{\odot}$ for the current total mass of stars; this value is comparable to the estimated mass within the central hundred parsec of the GC (Launhardt et al. 2002).

We synthesize stellar populations of ages from 0 to the assumed age of the Milky Way, 12 Gyrs, and integrate the stellar mass loss rate over all ages and initial masses. We find the total mass loss rate of the whole stellar population at 12 Gyrs to be $6.2 \times 10^{-3}\,M_{\odot}$/yr, and the AGB/PN-phase mass loss rate of the whole stellar population at 12 Gyrs to be $4.9 \times 10^{-3}\,M_{\odot}$/yr. We also find that the AGN/PN-phase mass loss rate does not vary significantly during a Galactic age between 3 and 12 Gyrs (see Figure 1). We adopt $5 \times 10^{-3}\,M_{\odot}$/yr as our canonical value for the gas replenishment rate in the inner nuclear bulge.

3. SIMULATION SETUP

We perform 3-dimensional hydrodynamic simulations of the evolution of the gas distribution that originates from the gas supply during the AGB/PN phase in the inner nuclear bulge of a Milky Way-like galaxy. We use the parallel N-body/SPH code GADGET-3 (Springel 2005)

and adopt numerical schemes developed to consider star formation, gas cooling and heating, and supernova feedback by Shin et al. (2014, 2017). The cooling function for gas by Spaans & Norman (1997) is implemented using a solar metallicity and initial temperature 10^4 K. The standard radiation strength used in our simulations is 100 G_0.

The gravitational potential of our galactic model includes a supermassive black hole with a mass of $4 \times 10^6\,M_\odot$ (Boehle et al. 2016), a nuclear star cluster that dominates the enclosed mass inside $r_g = \sim$10 pc as modeled by Merritt (2010), oblate versions of the nuclear stellar disk and galactic bulge as modeled by Rodriguez-Fernandez & Combes (2008), and a Miyamoto-Nagai model for the galactic disk with a total mass of $4 \times 10^{10}\,M_\odot$ and scale length and height of 3.5 kpc and 400 pc, respectively. We impose a softening length of 0.2 pc for the supermassive black hole to prevent unnecessarily small time steps.

Our simulations consider two different ways of supplying gas to the inner nuclear bulge, expressed here as two separate stages of our investigation. In the first stage, all gas particles are present from the beginning of the simulation; in the second stage, simulations begin without pre-existing gas particles which are created at a constant rate after the simulation starts. First-stage simulations are technically simpler and more straightforward, but they are less realistic and can be regarded as a test stage.

In the first stage, the standard initial parameters of our simulations are 10^4 gas particles, a total mass of $10^5\,M_\odot$, and a softening length of 0.3 pc. For the initial position and velocity distributions of the particles, we first create a self-consistent sphere with a desired density profile and isotropic velocity dispersion. Then, to obtain an initial cylindrical configuration, we remove particles that have a maximum 2-dimensional radial distance along the Galactic plane from the Galactic center larger than 180 pc and a maximum vertical deviation from the Galactic plane larger than 65 pc while being phase-mixed before the simulation. We impose a density profile of r_g^{-1} (we use a density slope of -1 here because the observed density slope between $r_g = 20$ and 100 pc is closer to -1 than -2; see, for example, Figure 14 of Launhardt et al. 2002).

We adopt a cylindrical configuration for the initial gas distribution because the interstellar gas considered here is from intermediate-age stars in the inner nuclear bulge, and the dominant portion of stars in this region are thought to have formed in the CMZ (Morris & Serabyn 1996). The CMZ is a rotating ring-like structure and the stars formed there are expected to diffuse mostly inward and vertically (Kim & Morris 2001) to form a cylinder-like structure. Indeed, the intermediate-age stars in the inner nuclear bulge observed by Schönrich et al. (2015) have a rectangular projected distribution on the sky with vertical and radial extents of $r_g \sim 50$ pc and ~ 150 pc, respectively. Likewise, the stellar population migrating inward and vertically from the CMZ must have some memory of orbital revolution; hence we adopt an initially rotating gas structure by enforcing 85%, instead of 50%, of gas particles to have the same sense of rotation as the Milky Way when projected onto the Galactic plane. This is achieved by flipping the sense of rotation for 70% of the particles that rotate retrograde.

For the second stage, we modified Gadget-3 to introduce new gas particles periodically throughout the simulation. In our standard second-stage simulation, new gas particles are added at a rate of $5 \times 10^{-3}\,M_\odot$/yr every ∼0.15 Myr, following the spatial and velocity distributions described above for the first-stage simulations. The mean mass of gas particles starts at $\sim 2.5\,M_\odot$ and steadily increases as simulations progress because we increase the mass of existing gas particles, instead of creating a new gas particle, when said particles are within a certain distance (10–30 pc) from the position to where a new gas particle is to be added.[4] The gas replenishment rate of $5 \times 10^{-3}\,M_\odot$/yr reflects the AGN/PN-phase mass loss rate calculated for the whole stellar population in the inner nuclear bulge in Section 2.

4. Simulation Results

Figure 2 shows the evolution of the gas distribution over 500 Myr in our standard first-stage simulation. The initial cylindrical structure flattens rapidly (within 3–5 Myrs) and a planar disk-like structure forms in the x-y plane. The planar structure is a result of the velocity dispersion of the gas particles, which originates from the velocity dispersion of the stars that replenish gas to the inner nuclear bulge, and the overall rotation in the initial gas distribution about the axis perpendicular to the Galactic plane. Any velocity difference between adjacent gas particles (or clumps) causes viscosity that reduces the bulk speed of gas, and this provokes gas particles to fall deeper into the Galactic potential. However, the overall angular momentum of the initial gas distribution causes the predominant inward migration of gas particles to occur vertically to the Galactic plane, which induces a planar configuration.

The vertical and radial extents of the disk-like structure approach an equilibrium after $T = 300$ Myr. Stars are formed in this structure at an SFR of order of $10^{-5}\,M_\odot$/yr, which is three to four orders of magnitude lower than that in the CMZ. The surface gas density in this structure, $\sim 10\,M_\odot/\mathrm{pc}^2$, is lower than that of the major ring in the CMZ, $30\,M_\odot/\mathrm{pc}^2$ (Kruijssen et al. 2014). We perform additional simulations with a larger total initial mass ($5 \times 10^5\,M_\odot$), smaller and larger softening lengths (0.1 and 1 pc), and a weaker degree of rotation (65 % of gas particles have the same sense of rotation) compared with our standard parameters. Nonetheless, the evolutionary aspects of gas distributions in these simulations are qualitatively similar to our standard simulation.

The gravitational potential becomes steeper at $r_g < 10$ pc due to the presence of the nuclear stel-

[4] The adopted particle addition time step (∼0.15 Myr) and distance criterion (10–30 pc) were practically the smallest acceptable values in terms of the wall-clock duration spent for the simulation.

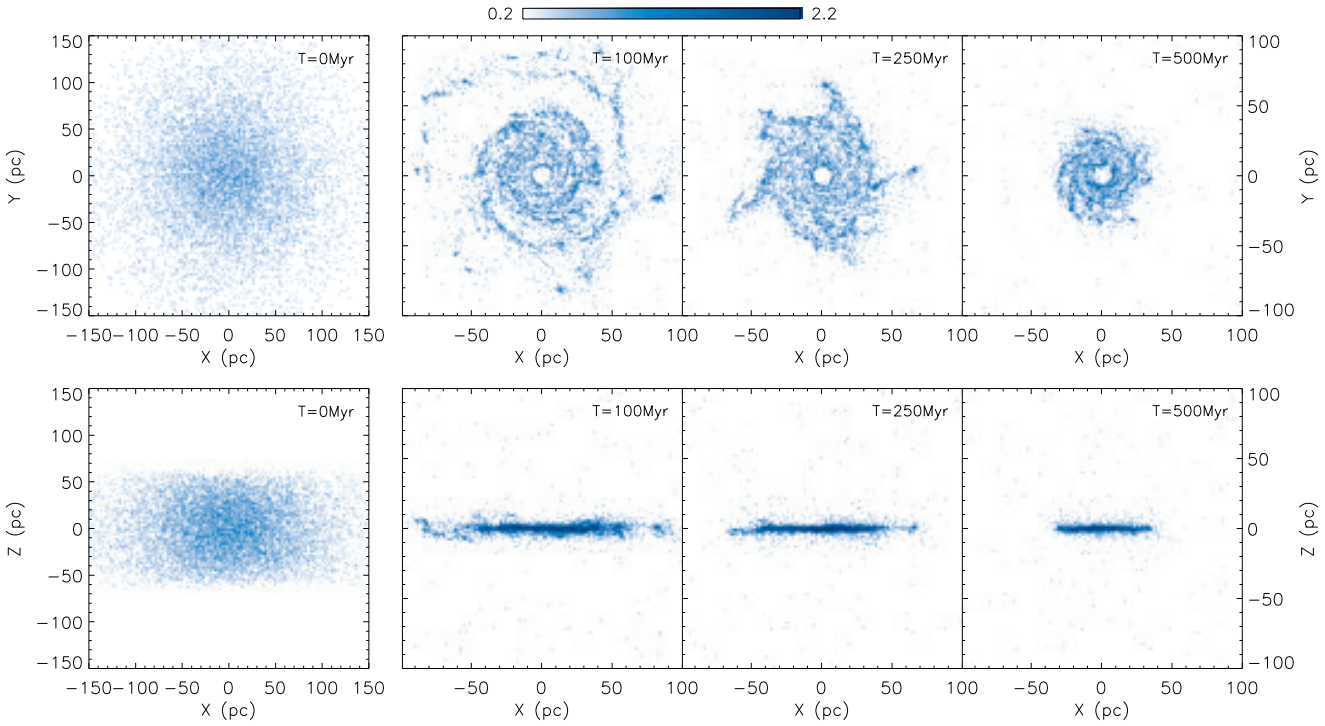

Figure 2. Surface density maps of gas particles from the standard first-stage simulation at T = 0, 100, 250, and 500 Myr. The color bar indicates the logarithmic column density in units of $M_\odot/\mathrm{pc}^2$.

lar cluster, hence a small number of gas particles is found inside $r_g = 10$ pc after $T{\sim}100$ Myr. A further infall of gas below 10 pc requires a loss of kinetic energy larger than that caused by the viscosity between gas clouds at different radii, which is inherently considered in hydrodynamic simulations like ours. Morris & Serabyn (1996) suggest several orbital energy loss processes aside from hydrodynamic viscosity, and among them, dynamical friction and magnetic viscosity are relevant to the region near $r_g = 10$ pc. Additionally, we suggest the interaction between the inner boundary of the gas disk near $r_g = 10$ pc and strong stellar winds from the central 1 pc or explosive events (supernova explosions) in the CND region as an additional orbital energy loss process. However, the further evolution of gas clouds near and below $r_g = 10$ pc is beyond the scope of the present study.

Our first-stage simulations clearly show that rotating, oblate distributions of gas particles in the inner nuclear bulge quickly evolve into highly flattened disky structures, where clumps can easily develop and infall to the vicinity of the CND. However, a shortcoming of our first-stage simulations is that gas particles are supplied to the simulation arena only at the beginning of simulations, whereas in reality, material is continuously supplied to the interstellar space by stars.

In the second stage, we simulate the evolution of gas that is constantly supplied to the inner nuclear bulge. Figure 3 shows the evolution of the gas distribution in the standard second-stage simulation over 300 Myr. The simulation initially starts with no gas, hence the first snapshot in Figure 3 is for $T = 10$ Myr. The total amount of gas in the simulation arena gradually increases as the simulation proceeds. As in the first-stage simulations, a disky structure quickly forms, but the constant gas replenishment prevents its radial extent from gradually decreasing. The total gas mass in the disk steadily increases and does not reach an equilibrium until the end of simulation, but the SFR in the gas disk reaches an equilibrium value of $\sim 2 \times 10^{-3}\, M_\odot/\mathrm{yr}$ after $T = 200$ Myr, which is ∼30 times higher than that in the standard first-stage simulation but still 1 to 2 orders of magnitude lower than the observed SFR in the CMZ. As in the first-stage simulation, the gas particles in the second-stage simulation can easily reach $r_g = 10$ pc, close to the CND.

There are two parameters controlling gas replenishment in our simulations: one controls how often new gas particles are added, the other controls how far the nearest gas particle must be in order to create a new gas particle instead of adding mass to existing gas particles. We varied these two parameters and the softening length but found that the simulation results are generally consistent to our standard second-stage simulation. Furthermore, we conclude that regardless if we implement continuous gas replenishment or not, the mass loss from stars in the inner nuclear bulge will form a low-density (relatively to the CMZ) gas disk in the Galactic plane with an inner boundary very close to the CND.

We note that the flattening timescale (few Myr) seen in our simulations may be too short to be realistic. Our simulations have 10,000–600,000 gas particles

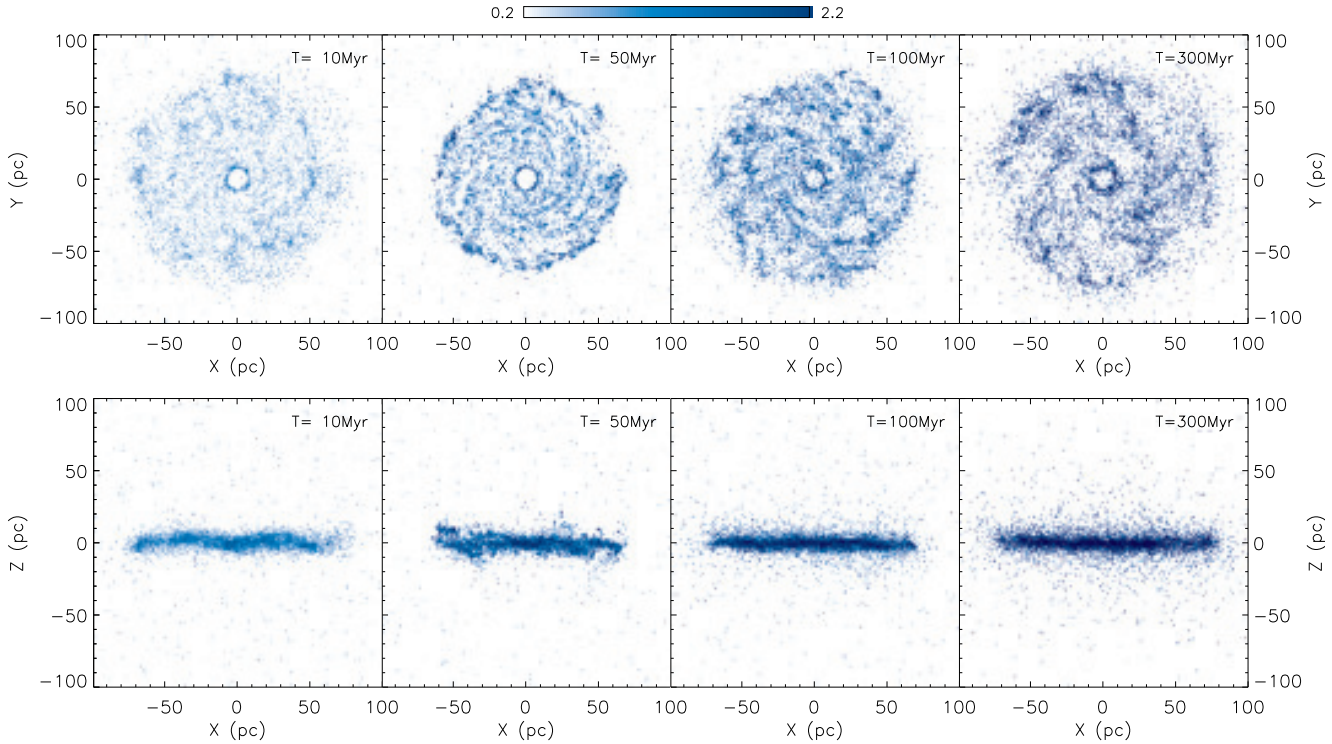

Figure 3. Surface density maps of gas particles from the standard second-stage simulation at T = 10, 50, 100, and 300 Myr. The color bar indicates the logarithmic column density in units of $M_\odot/\mathrm{pc}^2$.

outside the Galactic plane (vertical heights larger than 10 pc), but these numbers are not large enough to accurately describe detailed interactions between gas shells expanding (leaving) from thousands of stars during the AGB/PN phase at a given time. Although unrealistic, a large enough simulation that can trace the evolution of individual gas shells in the inner nuclear bulge may result in a longer flattening timescale, because a smaller portion of gas would collide and sink to the Galactic plane during a given time period. However, a replenished gas flow (or shell) will eventually meet another gas flow with a significantly different velocity vector (mostly in the vertical direction), loses orbital energy and sinks to the Galactic plane. Once a gas disk forms along the Galactic plane in the inner nuclear bulge, any gas flow with a considerable vertical orbital motion will collide with the gas disk within one orbit and quickly merge into the gas disk. To summarize, the flattening of the gas distribution in our simulations may occur more rapidly than what really happened in the inner nuclear bulge during the early phase of the Milky Way, but we expect that the eventual gas distribution found in our simulations provides a realistic description of the inner nuclear region for a major part of the Milky Way's lifetime.

5. Conclusions and Discussion

We have explored the plausibility of a mechanism that can deliver gas in the CMZ down to the CND area: diffusive inward migration of stars formed in the CMZ to the inner nuclear bulge, stellar mass loss from those stars (mainly during the AGN/PN phase), and formation of a gaseous disk whose inner boundary is at $r_g{\sim}10$ pc. Since the star formation in the CMZ is thought to have continued over the lifetime of the Milky Way, this mechanism is also expected to work continuously.

Some Galactic potential models may induce direct infall of gas from the CMZ down to the CND, but considering the relative radial extents of these two features, with the CMZ being ∼20 times more extended, direct infall is thought to be highly potential-dependent. Our new mechanism does not depend on the detailed gravitational potential of the Milky Way or any galaxy.

We have shown that the gas replenishment rate via stellar mass loss in the inner nuclear bulge (central ∼100 pc area of the GC) is at least $5 \times 10^{-3}\,M_\odot$/yr. Through 3-dimensional hydrodynamic simulations, we have shown that the majority of ejected gas from evolved stars eventually becomes a part of a low-density gas disk in the inner nuclear bulge.

Morris & Serabyn (1996) describe plausible mechanisms (dynamical friction and magnetic viscosity) that allow the gas clouds formed in the GC to migrate further inwards into the CND region. We infer that a further inward supply of gas below $r_g = 10$ pc occurs due to the interaction between the inner boundary of the gas disk obtained in our simulations and energetic events, such as supernova explosions and strong stellar winds from the CND and central parsec region.

The actual distribution of material between the CND (r_g = 2–7 pc) and the CMZ (r_g = 100–200 pc)

is highly uncertain because it is difficult to estimate the line-of-sight distance of gas observed in the GC. However, there are a few molecular structures that are thought to reside in this region: the 20 km/s cloud, the 50 km/s cloud, the Molecular Ridge, and the Western Streamer (e.g., Herrnstein & Ho 2005, Minh et al. 2013, Hsieh et al. 2017, and Armijos-Abendaño et al. 2019). Our simulation results are consistent with the observed gas structures because the gas clumps which form within the gas disk of our simulations can manifest as such structures. Energetic events, such as supernova explosions and strong stellar winds in the CND and the central parsec region, will disturb the orbital motions of gas clumps near the inner boundary of the gas disk seen in our simulations and may induce further infall of gas material down to the CND area (i.e., below $r_g = 10$ pc). We plan to investigate this possibility with hydrodynamic simulations in the future.

A recent simulation study suggests that some of the gas in the CMZ can directly fall to the central 50 pc region of the Galaxy, even without the presence of a secondary bar. The simulation by Tress et al. (2020) shows that the inclusion of gas self-gravity and a sub-grid prescription for supernova feedback can induce gas inflow below $r_g = 50$ pc at a rate of $\sim 0.03\,M_\odot$/yr. However, the mass inflow rate below $r_g = 50$ may strongly depend on the details of their prescription for supernova feedback and the adopted Galaxy potential model. It is not clear whether such mass inflow, owing to the gas self-gravity and supernova feedback in the inner nuclear bulge and the CMZ, is significant throughout the whole lifetime of the Milky Way.

ACKNOWLEDGMENTS

We are grateful to the anonymous reviewers for their helpful suggestions.

REFERENCES

Armijos-Abendaño, J., Martín-Pintado, J., Requena-Torres, M. A., et al. 2019, Herschel Water Maps towards the Vicinity of the Black Hole Sgr A*, A&A, 624, 112

Ballone, A., Mapelli, M., & Trani, A. A. 2019, A Common Origin for the Circumnuclear Disc and the Nearby Molecular Clouds in the Galactic Centre, MNRAS, 488, 5802

Boehle, A., Ghez, A. M., Schödel, R., et al. 2016, An Improved Distance and Mass Estimate for Sgr A* from a Multistar Orbit Analysis, ApJ, 830, 17

Debattista, V. P. & Shen, J. 2007, Long-lived Double-barred Galaxies from Pseudobulges, ApJ, 654, L127

El-Zant, A. A. & Shlosman, I. 2003, Long-lived Double-barred Galaxies: Critical Mass and Length Scales, ApJ, 595, L41

Erwin, P. 2004, Double-barred galaxies. I. A Catalog of Barred Galaxies with Stellar Secondary Bars and Inner Disks, A&A, 415, 941

Gallego, S. G. & Cuadra, J. 2017, Satellite Infall and Mass Deposition on the Galactic Centre, MNRAS, 467, L41

Gerhard, O. & Martinez-Valpuesta, I. 2012, The Inner Galactic Bulge: Evidence for a Nuclear Bar?, ApJL, 744, L8

Herrnstein, R. M. & Ho, P. T. P. 2005, The Nature of the Molecular Environment within 5 Parsecs of the Galactic Center, ApJ, 620, 287

Hsieh, P.-Y., Koch, P. M., Ho, P. T. P., et al. 2017, Molecular Gas Feeding the Circumnuclear Disk of the Galactic Center, ApJ, 847, 3

Hurley, J. R., Pols, O. R., & Tout, C. A. 2000, Comprehensive Analytic Formulae for Stellar Evolution as a Function of Mass and Metallicity, MNRAS, 315, 543

Jacob, R., Schonberner, D., & Steffen, M. 2013, The Evolution of Planetary Nebulae. VIII. True Expansion Rates and Visibility Times, A&A, 558, A78

Kim, S. S. & Morris, M. 2001, Spatial Diffusion of Stars in the Inner Galactic Bulge, ApJ, 554, 1059

Kroupa, P. 2002, The Initial Mass Function of Stars: Evidence for Uniformity in Variable Systems, Science, 295, 82

Kruijssen, J. M. D., Longmore, S. N., Elmegreen, B. G., et al. 2014, What Controls Star Formation in the Central 500 pc of the Galaxy?, MNRAS, 440, 3370

Laine, S., Shlosman, I., Knapen, J. H., & Peletier, R. F. 2002, Nested and Single Bars in Seyfert and Non-Seyfert Galaxies, ApJ, 567, 97

Lang, M., Holley-Bockelmann, K., Bogdanović, T., et al. 2013, Can a Satellite Galaxy Merger Explain the Active Past of the Galactic Centre?, MNRAS, 430, 2574

Launhardt, R., Zylka, R., & Mezger, P. G. 2002, The Nuclear Bulge of the Galaxy. III. Large-scale Physical Characteristics of Stars and Interstellar Matter, A&A, 384, 112

Lu, X., Zhang, Q., Kauffmann, J., et al. 2017, The Molecular Gas Environment in the 20 km s^{-1} Cloud in the Central Molecular Zone, ApJ, 839, 18

Maciejewski, W. & Sparke, L. S. 2000, Orbits Supporting Bars within Bars, MNRAS, 313, 745

Maciejewski, W. & Small, E. E. 2010, Orbital Support of Fast and Slow Inner Bars in Double-barred Galaxies, ApJ, 719, 622

Mapelli, M. & Trani, A. A. 2016, Modelling the Formation of the Circumnuclear Ring in the Galactic Centre, A&A, 585, A161

Martins, F., Genzel, R., Hillier, D. J., et al. 2007, Stellar and Wind Properties of Massive Stars in the Central Parsec of the Galaxy, A&A, 468, 233

Merritt, D. 2010, The Distribution of Stars and Stellar Remnants at the Galactic Center, ApJ, 718, 739

Minh, Y., C., Liu, H. B., Ho, P. T. P., et al. 2013, Green Bank Telescope Observations of the NH_3 (3, 3) and (6, 6) Transitions toward Sagittarius A Molecular Clouds, ApJ, 773, 31

Morris, M. & Serabyn, E., 1996, The Galactic Center Environment, ARA&A, 34, 645

Namekata, D., Habe, A., Matsui, H., & Saitoh, T. R. 2009, Mass Supply to Galactic Center due to Nested Bars in the Galaxy, ApJ, 691, 1525

Pfuhl, O., Fritz, T. K., Zilka, M., et al. 2011, The Star Formation History of the Milky Way's Nuclear Star Cluster, ApJ, 741, 108

Rodriguez-Fernandez, N. J. & Combes, F. 2008, Gas Flow Models in the Milky Way Embedded Bars, A&A, 489, 115

Schönrich, R., Aumer, M., & Sale, S. E. 2015, Kinematic Detection of the Galactic Nuclear Disk, ApJL, 812, L21

Shin, J., Kim, J., Kim, S. S., & Park, C. B. 2014, EUNHA: a New Cosmological Hydrodynamic Simulation Code, JKAS, 47, 87

Shin, J., Kim, S. S., Baba, J., et al. 2017, Hydrodynamic Simulations of the Central Molecular Zone with a Realistic Galactic Potential, ApJ, 841, 74

Spaans, M. & Norman, C. A. 1997, Cosmological Evolution of Dwarf Galaxies: The Influence of Star Formation and the Multiphase Interstellar Medium, ApJ, 483, 87

Springel, V. 2005, The Cosmological Simulation Code GADGET-2, MNRAS, 364, 1105

Tress, R. G., Sormani, M. C., Glover, S. C. O., et al. 2020, Simulations of the Milky Way's Central Molecular Zone – I. Gas Dynamics, MNRAS, 499, 4455

Wardle, M. & Yusef-Zadeh, F. 2008, On the Formation of Compact Stellar Disks around Sagittarius A*, ApJ, 683, L37